Electromigration Reliability of Open TSV Structures

Wolfhard H. Zisser[a], Hajdin Ceric[a,b], Josef Weinbub[a] and Siegfried Selberherr[a]
[a]Institute for Microelectronics, Technische Universität Wien, Gußhausstraße 27-29/E360, 1040 Wien, Austria
[b]Christian Doppler Laboratory for Reliability Issues in Microelectronics
Email: {zisser|ceric|weinbub|selberherr}@iue.tuwien.ac.at

***Abstract*—A study of electromigration in open through silicon vias is presented. The calculations are based on the drift-diffusion model for electromigration combined with mechanical simulations. The results show that the highest stresses are located at the aluminium/tungsten interfaces, near the region where the electrical current is introduced into the open through silicon vias, which happens to be the location of the highest current density at the interface. There, the electromigration induced degradation, e.g. void nucleation, is most probable to occur.**

I. Introduction

Three-dimensional (3D) integration is a promising approach for the development of systems with higher performance. Interconnections for 3D integrated circuits, though, include components not used in planar 2D architectures, such as through silicon vias (TSVs). Open through silicon vias introduced in [1] are a TSV concept in which the cylindrical structure is coated, rather than entirely filled with the conducting metal. The advantage of this technology, is that it can reduce the stress originating from the mismatched thermal expansion coefficients between the substrate and the TSV.

Electromigration (EM) addresses the material transport due to microscopic forces acting on mobile defects. These forces originate from the electric current and the electric field and cause therefore the flow of vacancies in current direction. The flow of material builds up stress in the interconnects, especially in the ones which carry high current densities, and leads to mechanical degradation, e.g. void nucleation or delamination [2].

In this work we investigate the possible EM reliability issues associated with this particular TSV technology. We use the drift-diffusion model for mass transport, in the aluminium part, which accurately treats the effects of EM. The results give the initial strain for a mechanical calculation to treat the stress in the whole structure. We simulate a segment of the geometry of the open TSVs as shown in Fig. 1. The result show that the highest stress is located at the outer surface of the aluminium cylinder along the interface between aluminium and tungsten. The highest vacancy concentration is found in the aluminium, in the region covered by the tungsten, which is therefore the region most sensitive to reliability issues.

II. Approach

The TSV geometry considered is shown in Fig. 1. Here, the tungsten, shown in red, forms an empty cylinder closed on the bottom side. Below that (not shown in figure) an aluminium plate is placed on which a solder pump is mounted to connect to other wafers. On the top side, an aluminium layer (shown in blue) forms a second empty cylinder, which overlaps with the inside, upper part of the tungsten cylinder wall. The upper side of the aluminium connects to the planar interconnect structure by a round plate as shown in Fig. 1. These open TSVs are different compared to the traditional copper TSVs which have their cylinders completely filled.

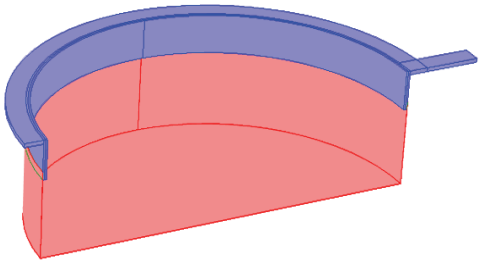

Fig. 1. TSV structure: Aluminium in blue and tungsten in red. The tungsten cylinder is shortened to 10% of the real length. For the simulated TSV the upper plate is removed.

In order to address EM in materials, two important microscopic forces must be considered to determine the material transport. The first is the so called direct force ($\vec{F}_{direct}$), caused by the the local electric field acting on the ionic atoms in the metal. The second is called the wind force ($\vec{F}_{wind}$), which is caused by the electrons scattered by the atoms in the metal [3]. The sum of these two forces determines the total force, as

$$\vec{F} = \vec{F}_{direct} + \vec{F}_{wind} = (Z_d + Z_w)e\vec{E} = Z^* e\vec{E}, \quad (1)$$

where Z_d and Z_w are the so called direct valence and wind valence, respectively, and Z^* is the effective valence, which describes the sensitivity to EM. $\vec{E}$ is the electrical field and e is the elementary electron charge.

For macroscopic modelling of the time evolution of the vacancy distribution C_v in a bulk material, a drift-diffusion model [4] with an additional generation/annihilation term G is used as

$$\frac{\partial C_v}{\partial t} = -\nabla \cdot \vec{J}_v + G. \quad (2)$$

The generation/annihilation term G, usually called Rosenberg-Ohring term [5], [6], is computed by

$$G = \frac{C_{v,eq} - C_v}{\tau}, \quad (3)$$

where $C_{v,eq}$ is the equilibrium concentration and τ is the characteristic relaxation time of the vacancy concentration.

The vacancy flux $\vec{J}_v$ is driven by three main forces, all of which are included in the bracket of the following equation

$$\vec{J}_v = -D_v \left(\nabla C_v - \frac{|Z^*|}{k_\mathrm{B}T} C_v \vec{E} + \frac{f\Omega}{k_\mathrm{B}T} C_v \nabla\sigma \right), \quad (4)$$

where k_B is the *Boltzmann* constant, T is the temperature, D_v is the diffusion coefficient of the vacancies, Ω is the atomic volume, and f is the relaxation factor. The first term in the bracket (first force) is a typical diffusion flux term due to different concentrations of vacancies. The second flux

978-1-4799-3929-9/14/$31.00

term is caused by the EM as described above, which is determined by the electric field in the structure. The third term is the flux due to different stresses in the material. A fourth flux term due to temperature gradients in the material could also be included, but is neglectable in this study, due to the homogenous temperature distribution in the aluminium and the tungsten.

For the stress term a solid mechanics simulation is required. The initial strain, which serves as an input to the solid mechanics simulation, is obtained by the following equation [7].

$$\frac{\partial \epsilon^v}{\partial t} = \Omega[(1-f)\nabla \cdot \vec{J}_v + fG] \quad (5)$$

The mechanical constraints were chosen as follows: The outside of the cylinder is surrounded by a silicon oxide/silicon substrate. Therefore, the position of the outer surface of the material is considered to be fixed. In the actual structures, inside the cylinder there is a thin silicon oxide layer, which is also taken into account in the calculations.

III. Results

The TSV structure includes surfaces connecting tungsten and aluminium. Since studies have shown that tungsten has a much lower sensitivity to EM [8], we focus our EM study on the aluminium structure on the top of the TSV, and include the tungsten only in the mechanical and electrical simulations.

The open TSV structure, which geometrically forms an arc, is shown on the left side of Fig. 2. On the top, an aluminium layer (shown in yellow) forms a second arc, which overlaps with the inside, upper part of the tungsten wall. The geometry considered in our calculations is a segment of this open TSV and shown on the right side in Fig. 2. The upper side of the aluminium (yellow) connects to the rectangular supply line aluminium interconnect, which is also included in the simulation domain. In the inner cylindrical surface of the TSV the aluminium and the tungsten are coated by a silicon oxide film (red).

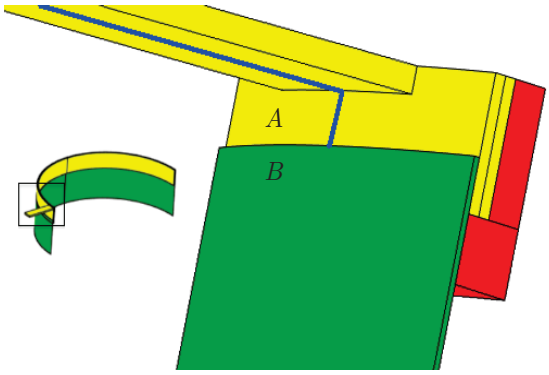

Fig. 2. TSV structure showing aluminum in yellow, tungsten in green, and silicon oxide in red. The blue line indicates a cut through the TSV for use in the subsequent figures.

For the mechanical stress simulations we use fixed boundary conditions on the aluminium surface labelled A and for the tungsten surface labelled B in Fig. 2. On the open surface of the oxide (red segment in Fig. 2), in the inner region of the arc, we employ open boundary conditions.

First we calculate the electrical current density in the considered geometrical structure, as shown in Fig. 3. The current flows through the aluminium interconnect (see arrow in Fig. 3), into the aluminium part of the TSV structure, and from there into the tungsten. The regions with the highest current density are shown in red. In the TSV part, a high current density is observed in the tungsten due to its thinner size compared to that of the aluminium section. At the corner of the interface of the two materials, however, a high current density is also observed (see zoomed-in inset). This current crowding at the corner at the very end of the interface is a result of the higher conductivity of aluminium and its larger thickness compared to tungsten, which provides a low resistance path for the current to flow to the corner of the interface, before it passes into the tungsten.

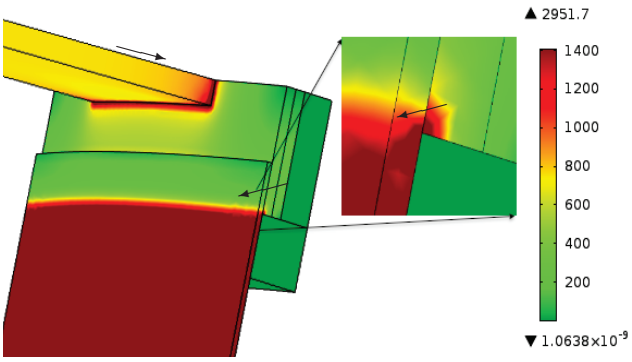

Fig. 3. Current density in the structure (A/cm^2). The inset is a zoom-in at the corner of the aluminium/tungsten interface.

After calculating the electrical current, we solve (2) together with the solid mechanics equations (5) to obtain the vacancy concentration in the aluminium, in order to determine the stress in the whole structure. Fig. 4 shows the relative change of the vacancy concentration ($c = (C - C_{eq})/C_{eq}$) compared to the equilibrium concentration C_{eq}, at the beginning of switching on the current. The figure is a cut through the blue line of Fig. 2. Most vacancies accumulate in the aluminium region, especially at the corner of the interface between aluminium and tungsten, where the highest current density is observed. The interface is blocking the vacancies and vacancy accumulation is created.

The corresponding tensile stress at $t = 1\,\mathrm{s}$ inside the TSV structure is shown in Fig. 5. In the aluminium region, where the vacancies are highly concentrated, higher tensile stress values are observed compared to the stress values in the tungsten region due to the presence of excess vacancies. At the interface of the two materials, the highest stress values are observed, attributed to the tendency of the aluminium to shrink compared to tungsten due to the difference in the vacancy concentration (c.f. Fig. 6).

An important observation, is that the results show a localized EM behaviour, extending only a few μm into the interconnect. Therefore EM studies can be restricted to these critical parts of the structures and can then be used for the prediction of the entire structure's resistance against EM degradation.

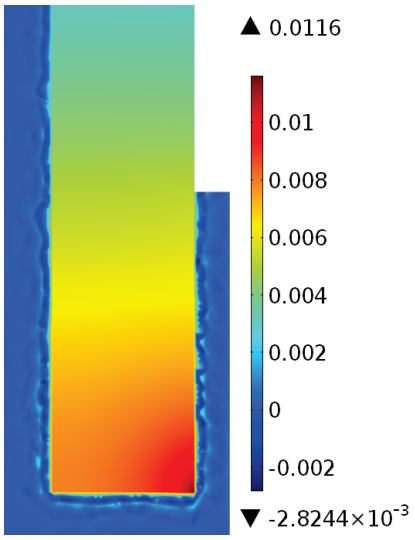

Fig. 4. Relative vacancy concentration change compared to the vacancy equilibrium concentration after $t = 1$s of current flow. A surface cut along the red line of Fig. 1 is shown. Red colour indicates the peak concentration.

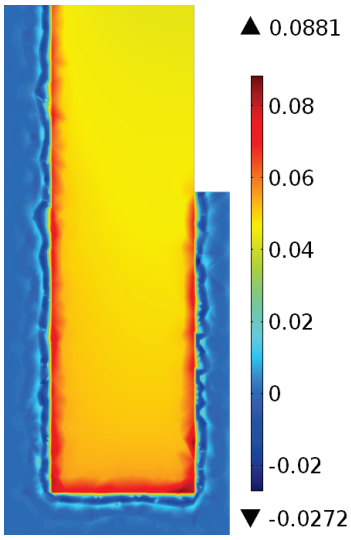

Fig. 6. Relative vacancy concentration change compared to the vacancy equilibrium concentration after $t = 10^6$s of current flow. A surface cut along the red line of Fig. 1 is shown. Red colour indicates the peak concentration.

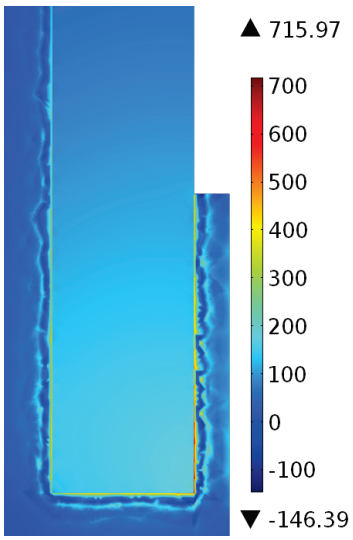

Fig. 5. Tensile stress (in Pa) after $t = 1$s of current flow. A surface cut along the red line of Fig. 1 is shown. Red colour indicates the peak tensile stress.

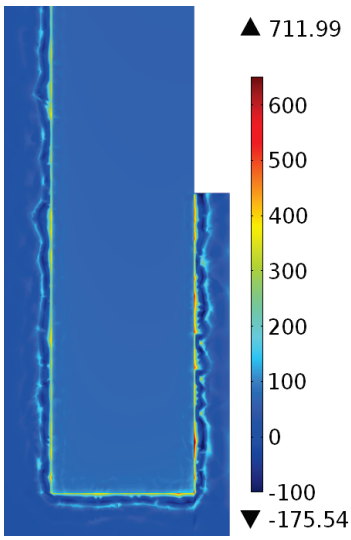

Fig. 7. Tensile stress (in MPa) after $t = 10^6$s of current flow. A surface cut along the red line of Fig. 1 is shown. Red colour indicates the stress peak.

For short times (e.g. 1 s) the stress build up is only driven by the displacement of vacancies due to the high current densities. After 10^5 s, however, the vacancies are less driven by the current and more by the tensile stress gradients. Fig. 6 shows the vacancy distribution after a longer time interval, again along the cut through the blue line of Fig. 2. Interestingly, the vacancies are more concentrated along the interfaces, both the aluminium/tungsten and aluminium/oxide interfaces. The highest tensile stress is also located along the aluminium/tungsten interfaces as shown by the red regions in Fig. 7.

The time evolution of the maximum stress in the structure (which is observed along the aluminium/tungsten interface) is shown in Fig. 8. Initially, the stress grows linearly in time proportional to the number of vacancies transported into the structure due to EM and annihilation in the aluminium. At longer times the stress growth rate decreases. The reason is that more stress is built up in the structure, the more it opposes the current density (see third term of (4)), which reduces the vacancy flow and therefore the stress build-up. Fig. 9 shows the maximum vacancy concentration versus time, which confirms the typical EM behaviour observed by Kirchheim [9]. In the beginning, the vacancy concentration increases, as vacancies accumulate in the aluminium. A quasi-steady state concentration is reached after a fairly short time [9]. As the vacancies recombine, the aluminium shrinks, which creates the stress accumulation observed in Fig. 9. At larger times, however, the vacancy concentration increases rapidly. This increase happens after a high stress magnitude is developed. In reality the tensile stress in the structure increases in such a way that void nucleation is triggered.

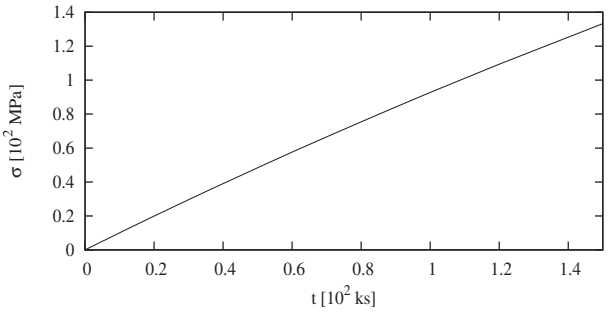

Fig. 8. Maximum stress versus time at the aluminium/tungsten interface.

Fig. 10 shows the stress development in time for different current densities. The stress build-up rises almost linear with the current density. When these results are fitted to Black's equation [10], with an appropriately chosen stress threshold as a failure condition, a current exponent of 0.74 is obtained shown in Fig. 11.

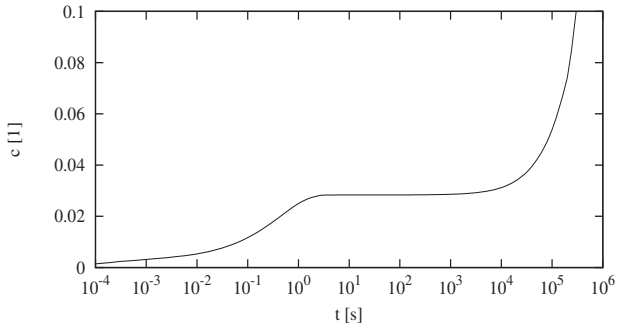

Fig. 9. Maximum relative vacancy density change versus time. Located at the aluminium/tungsten interface.

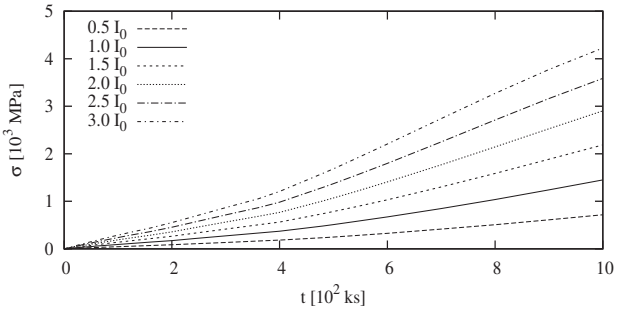

Fig. 10. Stress build up in the TSV for different current densities. I_0 is the current used for Fig. 8 and Fig. 9.

IV. Conclusions

Electromigration simulations in open TSVs were performed using the drift-diffusion model for mass transport, including solid mechanics simulations for stress and charge transport simulations for the current densities. We show that the largest stress in the material occurs along the aluminium/tungsten interface. The largest vacancy concentration in the via is observed in the aluminium, also near the regions surrounded by tungsten, where the stress is high. Finally, we show that EM has a localized behaviour, extending only a few μm into the interconnect, which indicates that EM studies can be restricted to these critical parts of the structures rather than the entire TSV.

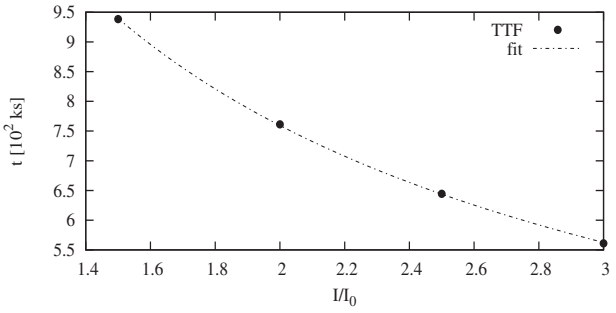

Fig. 11. Simulated TTF for different current densities. Broken line shows the exponential fitting of the results.

Acknowledgment

This work was supported by the Austrian Science Fund FWF, project P23296-N13.

References

1. J. Kraft, F. Schrank, J. Teva, J. Siegert, G. Koppitsch, C. Cassidy, E. Wachmann, F. Altmann, S. Brand, C. Schmidt, and M. Petzold, "3D sensor application with open through silicon via technology," *Proc. ECTC*, pp. 560–566, 2011.
2. I. A. Blech and C. Herring, "Stress generation by electromigration," *Appl. Phys. Lett.*, Vol. 29, No. 3, pp. 131–133, 1976.
3. R. S. Sorbello, "Microscopic driving forces for electromigration," *Proc. Mater. Research Soc. Symp.*, Vol. 427, pp. 73–81, 1996.
4. R. L. de Orio, "Electromigration modeling and simulation," Dissertation, Technische Universität Wien, June 2010.
5. R. Rosenberg and M. Ohring, "Void formation and growth during electromigration in thin films," *J. Appl. Phys.*, Vol. 42, No. 13, pp. 5671–5679, 1971.
6. H. Ceric, R. L. de Orio, J. Cervenka, and S. Selberherr, "A comprehensive TCAD approach for assessing electromigration reliability of modern interconnects," *IEEE Trans. Device Mat. Rel.*, Vol. 9, No. 1, pp. 9–19, 2009.
7. H. Ceric, R. Heinzl, C. Hollauer, T. Grasser, and S. Selberherr, "Microstructure and stress aspects of electromigration modeling," *Proc. AIP*, Vol. 817, No. 1, pp. 262–268, 2006.
8. J. Tao, K. Young, N. W. Cheung, and C. Hu, "Electromigration reliability of tungsten and aluminum vias and improvements under AC current stress," *IEEE Trans. Electron Devices*, Vol. 40, No. 8, 1993.
9. R. Kirchheim, "Stress and electromigration in Al-lines of integrated circuits," *ACTA Metall. Mater.*, Vol. 40, No. 2, pp. 309–323, 1992.
10. J. R. Black, "Electromigration: A brief survey and some recent results," *IEEE Trans. Electron Devices*, Vol. 16, No. 4, pp. 338–347, Apr 1969.